Available online at www.sciencedirect.com
ScienceDirect
Progress in Natural Science 18 (2008) 873–878
Progress in Natural Science
www.elsevier.com/locate/pnsc

Large eddies induced by local impulse at wall of boundary layer with pressure gradients

Changgen Lu [a,b,*], Weidong Cao [b], Yanmei Zhang [b], Jintao Peng [b]

[a] College of Atmospheric Science, Nanjing University of Information Science & Technology, Nanjing 210044, China
[b] College of Environmental Science and Engineering, Hohai University, Nanjing 210098, China

Received 2 January 2008; received in revised form 1 February 2008; accepted 1 February 2008

Abstract

Large eddies induced by local impulse at the wall with pressure gradients in the boundary layer was studied by direct numerical simulations. The results show that the amplitude evolution, the high and low speed stripes, the formation of streamwise vortices, the ejection and sweeping, inflexions and distortion at the mean velocity profiles, as well as other characteristics, are consistent with the experimental and other numerical results. It is also found that large eddies are easy to be excited with adverse pressure gradient in the boundary layer, and the growth of amplitudes, formation of streamwise vortices and the influencing area etc., are much larger than those with favorable pressure gradient in the boundary layer. In contrast, large eddies are hardly to be induced through local impulse disturbance at the wall with favorable pressure gradients in the boundary layer.

Keywords: Boundary layer; Pressure gradients; Impulse; Large eddies

1. Introduction

Transition is always an important topic in the field of fluid mechanics, which often occurs in ships, cars, planes, gas engines, etc. It is significant to forecast and control transition for ameliorating drive engines' motility and efficiency. Schubauer and Skramstad have experimentally proved secondary and higher order instability on the basis of linear disturbance wave's growth. Based on the weak nonlinear theory, Herbert conducted numerical simulations on the experiments of Saric et al., and successfully constructed the theory of secondary instability. Since the experiment of Klebanoff and Kanchanov et al. and the direct numerical simulation of Orszag and Fasel et al., it has been a classical and frequent method for transition by disturbance wave's instability growth [1]. Numerical simulation was conducted on the evolution of large eddies by Breuerl and Landahl, and many forms of eddy structure were obtained by using two pairs of inviscid reverse eddy structure as the large eddy initial models in the boundary layer [2]. The characteristics of large eddies are obtained by Jeong and Hussain numerically with steamwise eddies' model, and the results agree well with the experimental results [3]. Using hairpin vortices as initial disturbance, semi-streamwise vortices, semi-spanwise vortices and strong high shear layer are excited by Zhou et al. [4]. According to the structure of large eddies and the instable wave characteristics of transition in the experiment, resonant triad of hydrodynamic stability was adopted as large eddies' model by Jang et al. [5], and it was found that the asymmetrical disturbance could be excited and magnified easily. In channel flow, the growth of 3D spanwise disturbance wave was studied by Schoppa and Hussain with low speed stripe and the cause of inducing streamwise

* Corresponding author. Tel.: +86 13770755281; fax: +86 25 83786606.
E-mail address: lu678q@163.com (C. Lu).

1002-0071/$ - see front matter © 2008 National Natural Science Foundation of China and Chinese Academy of Sciences. Published by Elsevier Limited and Science in China Press. All rights reserved.
doi:10.1016/j.pnsc.2008.02.007

vortices and high shear layer, and the results were similar to the experimental results close to the wall [6]. The formation characteristics of large eddies in the Poiseuille flow and boundary layer have been numerically simulated by Spalart et al. [7] using the localized disturbance close to the wall as the initial flow. Katz et al. experimentally found that large eddies would be gradually diminishing in a boundary layer with favorable pressure gradients [8]. The occurrence and evolution of the large eddies induced by impulse at the wall of Blasius boundary layer had been numerically simulated by Singer [9]. Numerical simulation was conducted by Lu et al. on the evolution of large eddies in a turbulence boundary layer with pressure gradients with a period of instable wave as the initial model [10], and some useful results are obtained.

The cause of inducing large eddies is closely related to the Reynolds, wall temperature, shape, wall roughness, compressibility, pressure gradients and so on. Theoretical analysis was performed by Bertolotti on the effect of pressure gradients on the critical Reynolds in a boundary layer [11]. However, in the condition of large Reynolds, about the formation of large eddies, scale, shape and inside structure, there does not exist a clear conclusion. Recently, research on large eddies has been focused on the boundary layer with zero pressure gradients. However, in practice, most of the problems in the boundary layer are with adverse pressure gradients. Therefore, it is not only a theoretical problem but also a practical urgent problem to study the cause of large eddies induced by local impulse at the wall of boundary layer with different pressure gradients. Here, the cause and evolution of large eddies induced by local impulse at the wall of boundary layer with different pressure gradients have been studied by using direct numerical simulation.

2. Governing equations and numerical method

2.1. Governing equations and numerical method

The governing equations are the non-dimensionalized 3D incompressible Navier–Stokes equation and continuity equation:

$$\frac{\partial}{\partial t}\boldsymbol{u} + (\boldsymbol{u}\cdot\nabla)\boldsymbol{u} + (\boldsymbol{u}\cdot\nabla)\boldsymbol{u}_0 + (\boldsymbol{u}_0\cdot\nabla)\boldsymbol{u} = -\nabla p + 1/Re\cdot\nabla^2\boldsymbol{u} \quad (1)$$

$$\nabla\cdot\boldsymbol{u} = 0 \quad (2)$$

Here, ∇ is the gradient operators; ∇^2 is the Laplacian operators; $\boldsymbol{u}$, p are the disturbance wave's velocity and pressure, respectively; $\boldsymbol{u}_0$ is the basic solution of Falkner–Skan equation; $Re = U_e\cdot\delta/\upsilon = 3250$, where δ is the thickness of the inlet boundary layer, U_e is the velocity of inlet potential flow, and υ is the kinematic viscosity.

The procedures of direct numerical simulation of Eqs. (1) and (2) are as follows: a third-order mixed explicit–implicit scheme is employed for time discretization, and the space discretization is combined the higher accuracy compact finite differences of non-uniform meshes with the Fourier spectral expansion. Detailed information can be seen in Ref. [12]. The normalized time is 0.02.

2.2. Calculation region and boundary conditions

The calculation region is defined as follows:

- The streamwise: $0 \leqslant x \leqslant 120$; the spanwise: $-7.2 \leqslant z \leqslant 7.2$; the vertical: $0 \leqslant y \leqslant 6$; calculating grid: $\{x, y, z\} = \{200, 200, 32\}$.
- Inlet boundary condition: $x = 0$, $u = v = w = 0$, $\partial p/\partial x = 0$.
- Outlet boundary condition: $x = 120$, non-reflecting boundary condition.
- Boundary condition at the upper boundary; $y = 6$ $\partial u/\partial y = 0$ $\partial v/\partial y = 0$, $\partial w/\partial y = 0$, $p = 0$.

Boundary condition at the wall: $y = 0$, normalized impulse time $t \leqslant 10$, $v = A_0\sin[\pi(x - 2.5)/1.5]\cos[\pi z/3.6]$, which are distributed in the streamwise grid ($1 \leqslant x \leqslant 4$) and the spanwise grid ($-1.8 \leqslant z \leqslant 1.8$), where A_0 is the disturbance intensity of initial impulse, $A_0 = 0.014$, and the rest of the grids: $u = v = w = 0$; $\partial p/\partial y = 0$; the impulse at the wall is removed when $t > 10$. All of the grids are $u = v = w = 0$. Fig. 1 shows the initial distribution of vertical disturbance velocity without local impulse at the wall.

3. Results and analysis

The evolution of large eddies' amplitude induced by local impulse at the wall is shown in Fig. 2, in the condition of different pressure gradients ($\beta = -0.1$, -0.05, 0, $+0.05$, $+0.1$). The large eddies' amplitude is defined as:

$$A = \sqrt{|u|^2_{\max} + |v|^2_{\max} + |w|^2_{\max}} \quad (3)$$

Fig. 2 shows the evolution of amplitude with different pressure gradients. With the same settings of the given location, area and intensity of the initial local impulse at the wall, the evolution of the amplitudes of induced large eddies with different pressure gradients is not the same. With either favorable pressure gradients or zero pressure gradients at the wall of boundary layer, the evolution of amplitudes induced by local impulse usually increases at

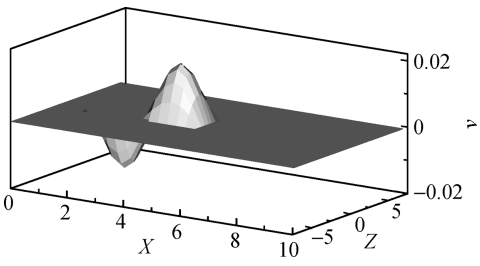

Fig. 1. Vertical disturbance velocity at the wall.

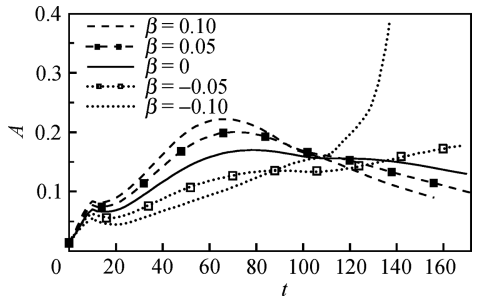

Fig. 2. The amplitudes evolution curves.

first, and then shrinks. But at the wall of boundary layer with adverse pressure gradients, evolution of the amplitudes induced by local impulse increases all along. The growth rate is related to the intensity of pressure gradients; the stronger the intensity is, the more dramatic the evolution is. Otherwise, the evolution is more inactive correspondingly. In the initial period of the evolution, the grow rate of large eddies induced by local impulse with favorable pressure gradients is larger than that with zero pressure gradients, and both are larger than that with adverse pressure gradients. The main reason is likely that the basic flow in the boundary layer with favorable pressure gradients is larger than that with adverse pressure gradients, secondly the effect of pressure gradients has not emerged fully, and the nonlinear effect is very weak and so on. Therefore, the condition of adverse pressure gradients can induce the formation of large eddies and accelerate the occurrence of turbulence whereas, the condition of favorable pressure gradients can restrain their formation, and stabilize the hydrodynamic flow.

Fig. 3 shows the variation of the largest local velocity profiles at $t = 60$, 100, 140 labeled by 1, 2, 3, respectively. In the process of nonlinear evolution and large eddies induced by local impulse, the velocity profile of the boundary layer has been changed at the wall of the boundary layer with different pressure gradients. According to the routine method in measuring velocity with hot-wire anemometer, the area with $|u| \geqslant 0.02$ is the core of large eddies, and the average velocity profile is presented there (Fig. 3). It is obvious that in a boundary layer with either favorable pressure gradients or adverse pressure gradients, the average velocity profile close to the wall is always much fuller than that of laminar flow, and the average velocity profile far away from the wall is always unsaturated, because of the existence of large eddies. As time goes on, the inflexion of average velocity profile is gradually coming into being in the boundary layer with adverse pressure gradients, and it becomes clearer and clearer. According to the theory of hydrodynamics stability, the average flow with such inflexion is unstable. The instable area and disturbance magnification coefficient included by the neutral curves have been greatly increased, which will accelerate the growth of large eddies in the end. It leads to the serious distortion of average velocity profile, and induces secondary instability, transition and so on. There exists obscure inflexion of average velocity profile in the boundary layer with favorable pressure gradients at first, but due to the effect of nonlinear evolution and the increasing of favorable pressure gradients, the inflexion will disappear quickly and the average velocity profile is much fuller than that with zero pressure gradients, which leads to hydrodynamics stability.

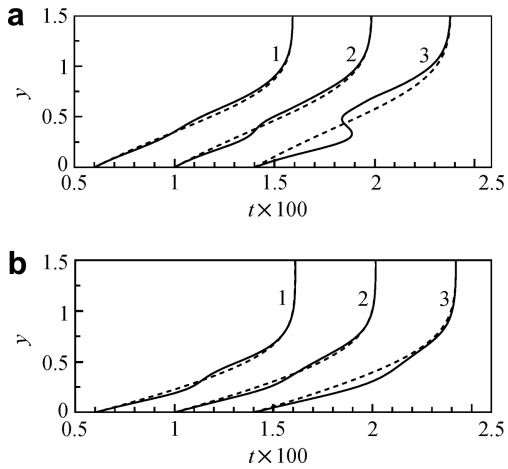

Fig. 3. Change of mean velocity profile with different pressure gradients. (a) $\beta = -0.1$; (b) $\beta = +0.1$. The dashed line is the velocity profile of Falkner–Skan, and the solid line is the average velocity profile involving large eddies.

In the generation and transportation of energy and transition in the boundary layer, the streamwise vortices play a vital role. Fig. 4(a)–(c) shows the velocity distributions of the streamwise vortices' maximum value in the boundary layer with adverse pressure gradients ($\beta = -0.1$) in the z–y plane at $t = 60$, 100 and 140, respectively. The streamwise vortices become more and more obvious, the intensity becomes stronger, and then different scales of the streamwise vortices come into being. With combination, avulsion, fragmentation and regeneration of the streamwise vortices again and again, the center of eddies goes up, and the influencing area is gradually diffused, and at last strong ejection and sweeping come into being besides the streamwise vortices. In addition, the size of streamwise vortices in the streamwise direction increases continuously. According to Biot–Savart theory, the vortex tube is lengthened in the streamwise direction, which will make the intensity amplified. At last the streamwise velocity and the spanwise velocity grow fast, the dramatic ejection and sweeping are formed, the strong shear layer is formed locally, and the flow is unstable. All these will accelerate the occurrence of turbulence. The velocity distributions of the streamwise vortices' maximum in the boundary layer with favorable pressure gradients ($\beta = +0.1$) in the z–y plane at $t = 140$ are shown in Fig. 4(d), there are no obvious streamwise vortices, that is, the flow tends to be stable.

Fig. 5 shows the streamwise disturbance velocity and vertical disturbance velocity distributions at the location of the maximum streamwise velocity in the boundary layer

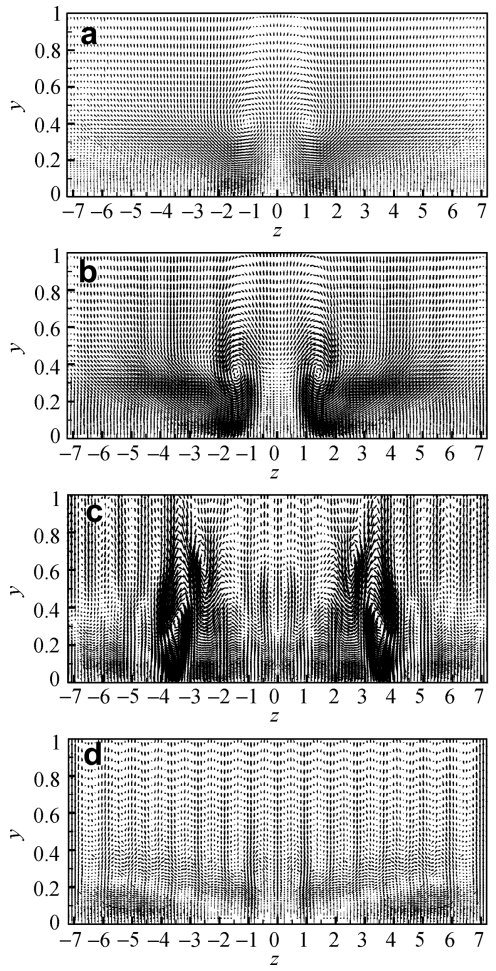

Fig. 4. Velocity distributions at Z–Y plane with different pressure gradients. (a) $t = 60$, $\beta = -0.1$; (b) $t = 100$, $\beta = -0.1$; (c) $t = 140$, $\beta = -0.1$; (d) $t = 140$, $\beta = +0.1$.

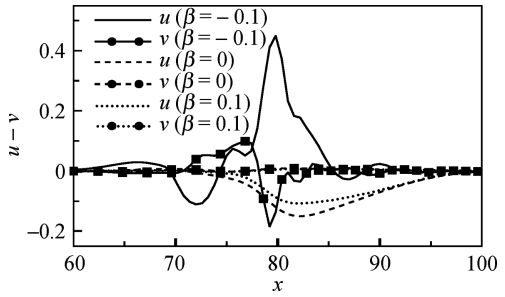

Fig. 5. Streamwise and vertical velocity profiles ($t = 140$).

with pressure gradients ($\beta = -0.1$, 0, $+0.1$) in the streamwise direction, respectively. As a whole, at the area with high speed flow where $u > 0$, corresponding to the area where the vertical velocity $v < 0$, the flow is the sweeping flow, whereas, at the area with low speed flow where $u < 0$, corresponding to the area where vertical velocity $v > 0$, the flow is the ejection flow. Both ejection flow and sweeping flow will accelerate Reynolds stress' fast growth. In the boundary layer with adverse pressure gradients, the velocity maximum of both the streamwise and the vertical is larger than that with favorable or zero pressure gradients. And the velocity maximum in the boundary layer with zero pressure gradients is larger than that with favorable pressure gradients. Because the physical characteristics of large eddies can be varied with the changing of the Reynolds and outer conditions, T–S wave might be found in some experiments. But it is not found in this study which is in agreement with the direct numerical simulation results of Singer [9].

The head and tail of streamwise position of large eddies are determined by $|u| \geqslant 0.02$ in the paper. Fig. 6 shows the head and tail of streamwise coordinate of large eddies in the boundary layer with different pressure gradients. The movement of large eddies in the boundary layer with adverse pressure gradients is slower than that with favorable and zero pressure gradients, and next is that the movement of large eddies in the boundary layer with zero pressure gradients is slower than that with favorable pressure gradients. The movement of large eddies is related to basic flow, the larger the velocity of the basic flow is, the faster the movement is, whereas the smaller the velocity of the basic flow is, the slower the movement is. Besides, the distance between the head and the tail denotes the expanding ability of large eddies. In Fig. 6, it is shown that though the movement of large eddies in the boundary layer with adverse pressure gradients is slower, the streamwise size is comparable to that with favorable and zero pressure gradients as time goes on. The reason may be that the spanwise vortices and the larger velocity gradient, that is, the capability of the viscosity and convective diffusion are larger than those with favorable and zero pressure gradients. This is consistent with Katz et al.'s experiment [8].

The contour of the streamwise disturbance velocity of large eddies induced by local impulse at the wall of boundary layer is shown in Fig. 7. It can be found that the scale of the sweeping flow is smaller than that of the ejection flow, but the vertical position of the ejection flow is higher than that of the sweeping flow. The results are in agreement with Praturi and Brodkey [13]. The sweeping flow is more concentrated and the pattern is fingerlike. In the condition of adverse pressure gradients, with the time development, the head of large eddies gradually goes up. The expanding

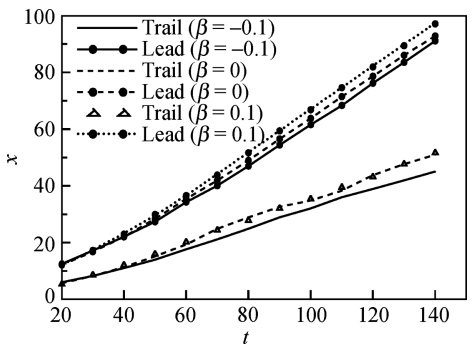

Fig. 6. The locations of large eddies' heads and tails.

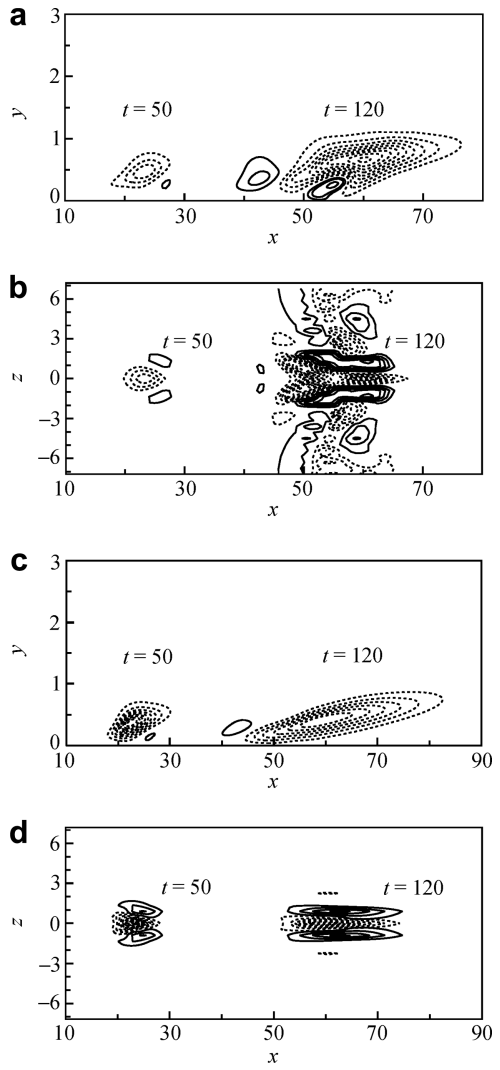

Fig. 7. Contour of streamwise velocity at the x–y and x–z planes (contour spacing 0.02). The dashed line is the slow speed flow ($u < 0$), the solid line is the high speed flow ($u > 0$). (a) $z = 0$, $\beta = -0.1$; (b) $y = 0.6$, $\beta = -0.1$; (c) $z = 0$, $\beta = +0.1$; (d) $y = 0.6$, $\beta = +0.1$.

capability of the spanwise and the vertical is obviously stronger than that with favorable pressure gradients, and the intensity of the ejection flow and the sweeping flow is also stronger than that with favorable pressure gradients. Due to the limit of the wall, the outer high speed flow is coming into the inner because of the sweeping flow. Momentum and energy will diffuse around inevitably. This is the main reason for the spanwise size in the boundary layer with adverse pressure gradients being larger than that with favorable pressure gradients. And the size of the ejection flow is much bigger than that of the sweeping flow. This is consistent with Lian et al.'s results [14]. With either the favorable or the adverse pressure gradients, the high and low speed stripes vary continuously. In the boundary layer with adverse pressure gradients, a strong shear layer is formed between the high and low speed stripes. As a result, different scales of streamwise and spanwise vortices are formed. Provided that the spanwise average interval between non-dimensional high and low speed stripes is defined by $\lambda^+ = \lambda u_\tau / v$, where $u_\tau = \sqrt{\tau_w/\rho}$ is the shear velocity, then the average interval between high and low speed stripes in the boundary layer with adverse pressure gradients ($\beta = -0.1$) is about 90, and it is about 70 with favorable pressure gradients ($\beta = +0.1$). The average interval between high and low speed stripes in the boundary layer with adverse pressure gradients is larger, which is in agreement with Kline's result that the average interval between high and low speed stripes is $\lambda^+ \approx 100$ at the wall of turbulence boundary layer in experiments [15]. Kline also found that the streamline began to break down when the position of the ejection flow ($y^+ = yu_\tau/v$) reached about 30. Klebanoff [16] measured the distribution of turbulence energy in the positive vertical direction by hot-wire anemometer with most burst occurrence in $y^+ = 10$–40. The maximum position of the ejection flow in the boundary layer with favorable pressure gradients is approximate

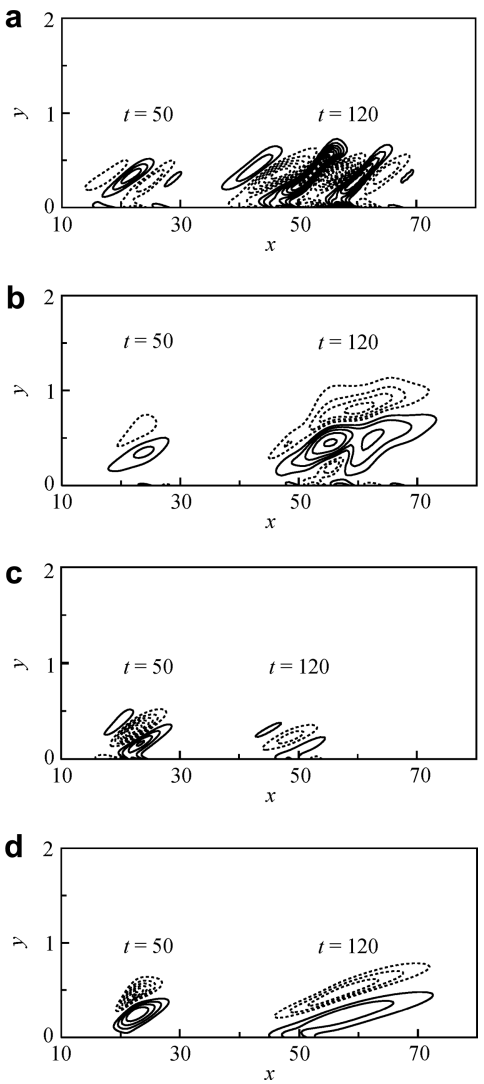

Fig. 8. Contour of streamwise and spanwise vortices. The solid lines represent the positive value, the dashed lines for the negative value, and the contour space is 0.015. (a and b) $\beta = -0.1$; (c and d) $\beta = +0.1$.

$y^+ = 30$, and that with favorable pressure gradients is approximate $y^+ = 40$ in this study.

Fig. 8 shows the contour of the maximum positions of the streamwise and spanwise vortices in the boundary layer ($\beta = -0.1, +0.1$) at $t = 50, 120$, respectively. In the boundary layer with adverse pressure gradients, the intensity of both the streamwise and the spanwise vortices gradually increases with time; in the boundary layer with favorable pressure gradients, though at $t = 120$ the area of the spanwise vortices is larger than that at $t = 50$, the intensity does not increase; on the contrary it becomes diminished, and the intensity of the streamwise vortices also decreases. Besides, the declining streamwise vortex tube reaches the wall in the boundary layer with adverse pressure gradients, and its head gradually goes up. With the characteristics of hairpin vortex's leg, the occupied area gradually increases. The streamwise vortices show the inerratic distribution, and these results are similar to the evolution of large eddies reviewed by Lian [14].

4. Conclusions

Numerical simulations are conducted on the nonlinear evolution of the large eddies at the wall of boundary layer with pressure gradients, and the conclusions are summarized as follows:

(1) With the time development in the boundary layer with adverse pressure gradients, large eddies are much easier exited, and the disturbance amplitudes of large eddies are larger than that with favorable and zero pressure gradients. The stronger the intensity of adverse pressure gradients is, the more dramatic the evolution is, but the evolution is much gentle correspondingly.
(2) With the time development, the inflexion of average velocity profile gradually comes into being in the boundary layer with adverse pressure gradients, and it becomes clearer and clearer, which leads to the serious distortion of the average velocity profile.
(3) In the evolution process of the large eddies in the boundary layer with adverse pressure gradients, the large eddies in the vertical and the spanwise direction have been gradually expanded, and the influencing area has also become larger, these will induce the streamwise vortices obviously.

In the spatial evolution of large eddies induced by local impulse in the boundary layer with adverse pressure gradients, there are always the high and low speed stripes. Strong shear layer is formed between the stripes, and the size of streamwise vortices in the streamwise direction increases continuously. Therefore, the Reynolds stress grows quickly, the dramatic ejection and sweeping are formed, and the flow is unstable. All these will accelerate the occurrence of turbulence.

Acknowledgements

This work was supported by National Natural Science Foundation of China (Grant Nos. 10672052 and 1027204) and the Natural Science Foundation of Jiang Su province of China (Grant No. BK2007178).

References

[1] Rempfer D. Low-dimensional modeling and numerical simulation in simple shear flows. Annu Rev Fluid Mech 2003;35:229–65.
[2] Breuerl KS, Landahl MT. The evolution of a localized disturbance in a laminar boundary layer. Part 2, strong disturbance. J Fluid Mech 1990;220:595–621.
[3] Jeong J, Hussain F, Schoppa W, et al. Coherent structures near the wall in a turbulent channel flow. J Fluid Mech 1997;32:185–221.
[4] Zhou J, Adrian RJ, Balachandar S, et al. Mechanisms for generating coherent packets of hairpin vortices in channel flow. J Fluid Mech 1999;387:353–81.
[5] Jang PS, Benney DJ, Granl RL. On the region of streamwise vortices in a turbulent boundary layer. J Fluid Mech 1986;169:109–31.
[6] Schoppa W, Hussain F. Coherent structures generation in near-wall turbulence. J Fluid Mech 2001;453:57–108.
[7] Spalart HP, Kim J. Numerical simulations of turbulent spots in plane Poiseuille and boundary layer flow. Phys Fluids 1987;30(4):2914–8.
[8] Katz Y, Seifert A, Wygnsnski I. On the evolution of the turbulent spot in a laminar boundary layer with a favourable pressure gradient. J Fluid Mech 1990;221:1–22.
[9] Singer BA. Characteristics of a young turbulent spot. Phys Fluids 1996;8(2):509–21.
[10] Lu LP, Li ZR. Analysis of coherent structures in a turbulent boundary layer with pressure gradients. Eng Sci 2002;4(11):50–6.
[11] Bertolotti FP, Herbert Th, Sparlart PR. Linear and nonlinear stability of the Blasius boundary. J Fluid Mech 1992;242:441–74.
[12] Lu CG, Cao WD, Qian JH. A study on numerical method of Navier–Stokes equations and nonlinear-evolution of the coherent structure in a laminar boundary layer. J Hydrodyn B 2006;18(3):110–6.
[13] Praturi AK, Brodkey RS. A stereoscopic visual study of coherent structures in turbulent shear flows. J Fluid Mech 1978;89:251–72.
[14] Lian QX. Experimental studies on coherent structures in turbulent boundary layers. Adv Mech 2006;3:373–88.
[15] Kline SL, Reynolds WC, Schraub FH, et al. The structure of turbulent boundary layers. J Fluid Mech 1967;30:741–74.
[16] Klebanoff PS. Characteristics of turbulence in a boundary layer with zero pressure gradient. NACA Report 1955; 1247.